Numerical simulations on blast wave around the small-scale model of subsurface magazine

Yuta Sugiyama*†, Tomohiro Tanaka**, Akiko Matsuo**, Tomotaka Homae***, Kunihiko Wakabayashi*, Tomoharu Matsumura*, and Yoshio Nakayama*

*National Institute of Advanced Industrial Science and Technology (AIST),
  Central 5, 1−1−1 Higashi, Tsukuba, Ibaraki 305−8565, JAPAN
  Phone : +81−29−861−0552
†Corresponding author : yuta.sugiyama@aist.go.jp

**Keio University, 3−14−1 Hiyoshi, Kohoku−ku, Yokohama, Kanagawa 223−8522, JAPAN

***Toyama National College of Technology, 1−2 Ebie−neriya, Imizu, Toyama 933−0293, JAPAN

Abstract

This paper visualizes explosion phenomena in a small-scale subsurface magazine model that is constructed in the ground to mitigate a blast wave, which presents a physical hazard to persons and property. Numerical simulation models the previous experiment by Homae *et al*. and gives observations of detailed phenomena. From the viewpoint of safety assessment, evaluating the strength of a blast wave on the ground is important. The simulated data agree with the results of the previous experiment. As compared with the case of a hemispherical surface explosion, the peak overpressure of the subsurface explosion is clearly mitigated. Our study showed that 30% of the high explosive energy contributes to the propagation of the blast wave to the open space. In the circular pipe, a shock wave reflects off the wall several times, which causes the multi-dimensional shock wave front with a triple point and disturbed flow behind it. Although a non-uniform blast wave appears near the exit, the spherical blast wave finally expands to the outside the subsurface magazine model far from the exit.

Keywords : numerical simulation, subsurface magazine, mitigation, blast wave

1. Introduction

High explosives are used widely in industrial operations such as mining and blasting excavation because even a small amount of explosive releases powerful energy instantly. However, unexpected heating in the chamber of a magazine can cause detonation of high explosives and the release of high-pressure gas. In the process of gas expansion, the generated blast wave is a hazard to people and has the potential to cause extensive damage to property. In order to store high explosives safely, some types of explosive magazines are now regulated in Japan, including above-ground magazines and igloo-type magazines. However, recently, more and more magazines are constructed in limited spaces. In order to make use of limited space, it is necessary to develop a new type of magazine that can reduce the distance between the magazine and residential areas. Subsurface magazines have been proposed as a suitable type of magazine[1]−[4].

A vertical elevator is used as an exit from the storage chamber. This structural advantage brings a mitigation of the blast wave and reduction of fragments generated by explosion. Sugiyama *et al*.[5] conducted the numerical simulation of the explosion inside the simplest two-dimensional underground structure, and showed that when the size of the underground structure is larger, blast wave gives much mitigation effect on the ground. Saburi *et al*.[1],[2] described experimental studies on debris hazards and the ground vibration from explosion in subsurface magazines using the high explosive around 10 kg. Homae *et al*.[3] conducted experiments with a small-scaled subsurface magazine using the high explosive around 1 g. The experimental results showed obvious blast wave

mitigation, as compared with the case of surface explosion. Numerical simulation can provide much available data, supporting the results of explosion experiment and providing quantitative investigation of the mitigation mechanism. This paper models the previous experiment by Homae *et al*.[3] We evaluate the peak overpressure of the ground around a subsurface magazine and show flow characteristics in the small-scale subsurface magazine.

2.　Numerical methods

The governing equations are the compressible Euler equations in generalized coordinates in two-dimensional axisymmetric assumption and in three-dimension. For closure of these equations, the fluid is modeled as an ideal gas with constant specific heat ratio, $\gamma = 1.4$, and all diffusive effects are neglected. These equations are discretized using the second-order HLL (Harten-Lax-Leer) -HLLC (Harten-Lax-Leer for Contact) scheme[6)–8)] by MUSCL (Monotonic Upstream-centered Scheme for Conservation Laws) interpolation with minmod limiter. The switching of the HLL and HLLC schemes is determined by the pressure differences between a grid point and the other points around it. The two-stage Runge-Kutta method is used for time integration. Since the previous study[9] showed that the distance scaled by the mass of explosive determines the characteristics of the blast wave, our data, as well as those from the experiments of Homae *et al*.[3], incorporate a scaled distance Z, m kg$^{-1/3}$.

First, we conduct a hemispherical explosion with the compressible two-dimensional axisymmetric Euler equations to verify our numerical methods and conduct a grid convergence study by comparison with the empirical curve of Kingery and Bulmash[9]. In the present study, an explosion is modelled by setting up hemispherical high-pressure air. It has the same energy as 1 kg of TNT (4.2 MJ kg^{-1}). In the radial direction, three grid spacings of 0.0025, 0.005, and 0.02 m kg$^{-1/3}$ are distributed uniformly in the calculation domain. Figure 1 shows the peak overpressure distribution of hemispherical explosion in the case of the present study, along with the empirical
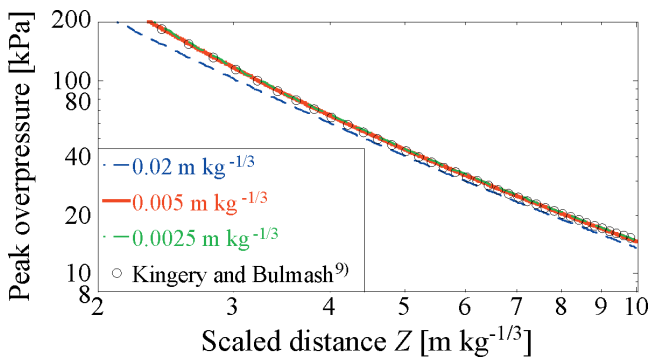
Figure 1　Peak overpressure distributions of the hemispherical explosion in the present study and the empirical curve of Kingery and Bulmash[9]. Numerical data are obtained by two-dimensional axisymmetric calculation with three grid spacings of 0.02, 0.005, and 0.0025 m kg$^{-1/3}$. The horizontal axis indicates the scaled distance Z m kg$^{-1/3}$.
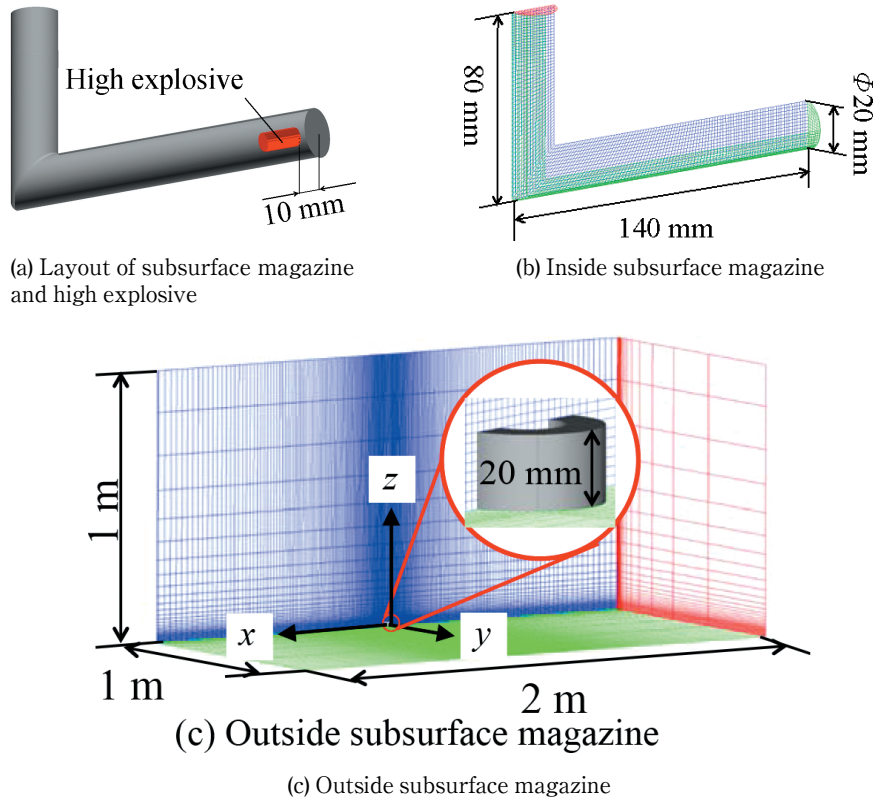
formula of Kingery and Bulmash. In Figure 1, the results of the present calculations show good agreement with the empirical curve when the grid spacing is smaller than 0.005 m kg$^{-1/3}$. We will calculate the subsurface explosion under the condition that the grid spacing is set to less than 0.005 m kg$^{-1/3}$.

This paper models the experiments of subsurface and surface explosion conducted by Homae *et al*.[3] The high-energy air for subsurface and surface explosion is the same as that of high explosive (PETN, 5.6 MJ kg^{-1}) used in the previous experiment. Figure 2 shows (a) the layout of the subsurface magazine and high explosive and the grids of two zones, (b) inside and (c) outside the subsurface magazine with boundary conditions in the case of the subsurface explosion. The subsurface magazine model is a pipe with a diameter of 20 mm that bends up to the ground at the end of the horizontal chamber as shown in Figures 2 a and 2b. As shown in Figure 2a, an explosion occurs 10 mm away from the wall along the central axis of the chamber, and a high explosive is modeled as cylindrical high-energy air. In the present sturdy, mass of PETN is fixed as 1.0 g. Its shape is a cylinder whose ratio of length and diameter is 2. In the present study, the origin of the scaled distance is the center of the vertical chamber on the ground. The grid spacing at $y = 0$ and $z = 0$ is set to be less than 0.005 m kg$^{-1/3}$, as discussed above, in order to accurately evaluate the peak overpressure on the ground as shown in Figure 2c. Colored boundary conditions are described below. For the symmetric calculations, mirror boundary condition is adopted in a blue region. A slip wall and an outflow conditions for other boundaries are set in the green and red regions (only described at $x = -1$ m) in Figures 2b and 2c, respectively. Physical values of the red boundary in Figure 2b connect and interpolate the exit of the subsurface magazine on the ground as shown in the inset of Figure 2c.

In the case of surface explosion, two-dimensional axisymmetric calculation is conducted. In the radial direction, constant grid spacing of 0.005 m kg$^{-1/3}$ is distributed uniformly in the x and y directions. The explosion center of hemispherical high-energy air (5.6 kJ and 10 mm in diameter) is set at the origin.

3.　Results and discussions

For safety analysis, we focus on the peak overpressures and propagation of the blast wave on the ground. Figure 3 shows the peak overpressure distributions on the ground surface ($x \geq 0$, $y = 0$, and $z = 0$) in the case of the surface explosion (blue) and the subsurface explosion (red) when 1.0 g of high-energy air. The horizontal axis indicates the scaled distance Z. Plots and curves denote the results by the experiment and the present simulations, respectively. The peak overpressures decrease as the shock wave moves away from $Z = 0$. Our numerical data shows that the peak overpressure at $Z = 5$ m kg$^{-1/3}$ in the case of surface explosion differs from that of the experiment about 30 %, and that other data agree with those of the experiment within 10 %. The peak overpressure in the case of subsurface explosion is notably mitigated, and

(a) Layout of subsurface magazine and high explosive

(b) Inside subsurface magazine

(c) Outside subsurface magazine

Figure 2   (a) Layout of the subsurface magazine and high explosive, and the grids of two zones, (b) inside and (c) outside the subsurface magazine with boundary conditions and in the case of the subsurface explosion.
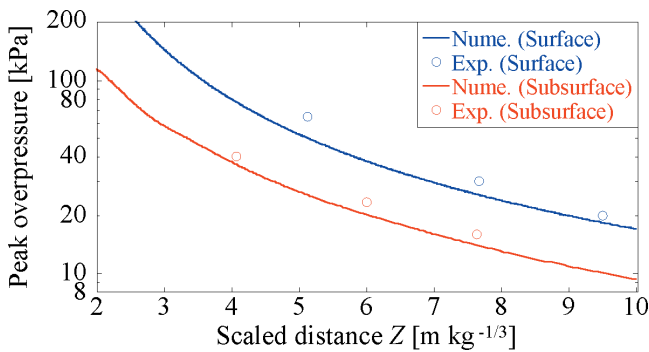
Figure 3   Peak overpressure distributions on the ground surface ($x \geq 0$, $y = 0$, and $z = 0$) in the case of the surface explosion (blue) and the subsurface explosion (red) when $1.0\,g$ of high-energy air. The horizontal axis denotes the scaled distance Z m $kg^{-1/3}$.

becomes half that in the case of surface explosion.

To discuss the blast wave generation and propagation inside and outside the subsurface magazine, we utilize the flow patterns as shown in Figures 4 and 5. Figure 4 shows the pressure distributions in central cross section of the subsurface magazine. In Figure 4a, the explosion generates shock waves that propagate in the horizontal circular pipe. The rightward and leftward shock waves propagate from the explosion center. The leftward shock wave reflects on the left-end wall, which generates the high-pressure region near the left-end wall in Figure 4a. In Figure 4b, the rightward shock wave diffracts at the corner of the subsurface magazine and weakens. The shock wave reflected at the left-end wall runs after the

rightward shock wave in the horizontal pipe. In Figure 4c, the high-pressure region appears near the right-end wall of the horizontal pipe, since the rightward shock wave reflects off the right-end wall. In Figure 4d, the rightward shock wave propagates to the vertical pipe and reflects off the wall of the vertical pipe. This creates a triple point, where three shock waves meet ; incident shock, reflected shock, and Mach stem, on the shock front. The rightward shock wave moves upward to the exit of the subsurface magazine and expands as a blast wave from the exit of the subsurface magazine. The shock wave reflected at the left-end wall does not reach and therefore does not affect the rightward shock wave.

Figure 5 shows (a) the pressure distributions in central cross section near the exit of the subsurface magazine and (b) blast wave shape near the subsurface magazine at 60 μ s. The high-pressure gas is released from the subsurface magazine to open space. The pressure shows non-uniform distribution due to reflections of the rightward shock wave in the vertical pipe of the subsurface magazine. The blast wave comes to approximate a hemispherical shape. Figure 6 shows the pressure distributions in central cross section near the exit of the subsurface magazine at 260 μs. The hemispherical blast wave spreads and reaches the ground surface. Since the interference between the shock wave and the ground surface causes generation of the triple point, the pressure near the ground surface becomes higher as shown in the inset of Figure 6.

Now we discuss the mitigation effect of the blast wave in the case of the subsurface explosion. We focus on the strength of the rightward shock wave in Figure 4 from the
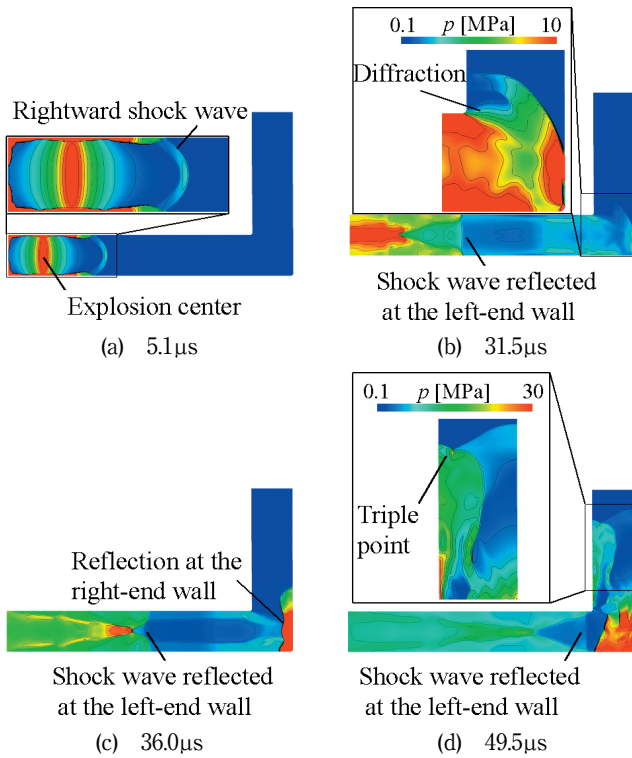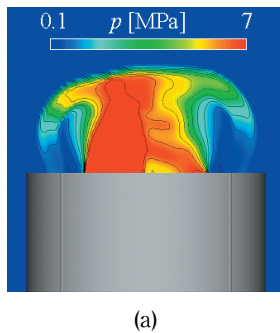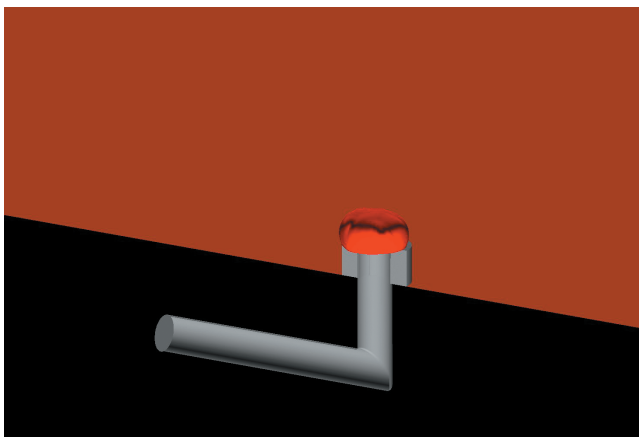
Rightward shock wave

Explosion center

(a)   5.1μs

Diffraction

Shock wave reflected
at the left-end wall

(b)   31.5μs

Reflection at the
right-end wall

Shock wave reflected
at the left-end wall

(c)   36.0μs

Triple
point

Shock wave reflected
at the left-end wall

(d)   49.5μs

Figure 4   Pressure distributions in central cross section of the subsurface magazine.

(a)

(b)

Figure 5   (a) Pressure distributions in central cross section near the exit of subsurface magazine, (b) Blast wave near the subsurface magazine at $60 \, \mu$s.

viewpoint of energy evaluation of the high explosive, whose initial energy is defined as E_0.

As shown in Figure 4c, the rightward shock wave diffracts at the corner. This indicates that a part of E_0 is distributed to the propagation of the rightward shock wave and the generation of the blast wave at the exit of
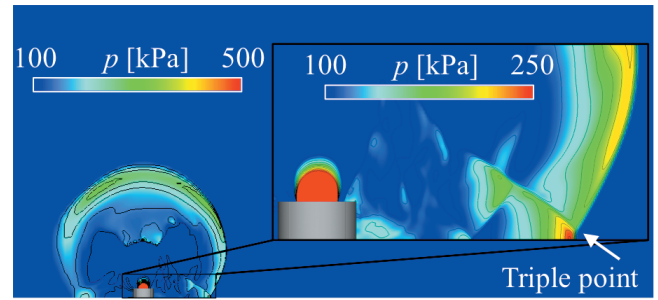

Triple point

Figure 6   Pressure distributions in central cross section near the exit of the subsurface magazine at $260 \, \mu$s.
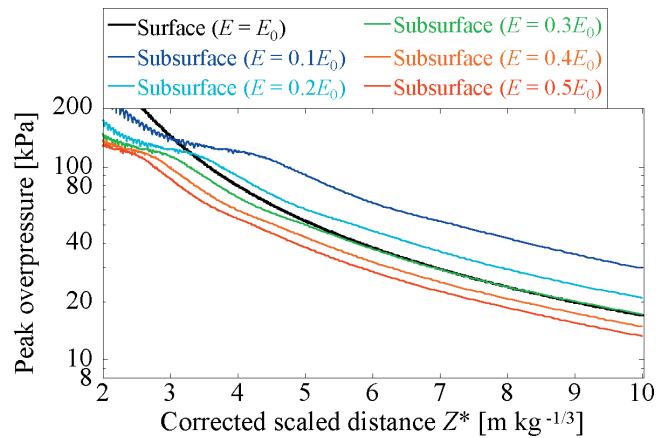

Figure 7   Peak overpressure distribution on the ground surface. The horizontal axis denotes the corrected scaled distance $Z^* = Z/(E/E_0)^{1/3} \, \mathrm{m \, kg^{-1/3}}$.

the subsurface magazine. Therefore, to estimate the blast wave strength, the peak overpressure distributions are reevaluated using a corrected scaled distance $Z^* = Z/(E/E_0)^{1/3}$ taking into account the energy loss by the subsurface magazine. Here, E_0 denotes the initial energy of the high explosive (1.0 g of PETN). E denotes a part of the initial energy E_0 and contributes to the generation of the blast wave. Figure 7 shows the peak overpressure distributions of the surface explosion and the subsurface explosion. The horizontal axis denotes the corrected scaled distance $Z^* = Z/(E/E_0)^{1/3}$, and the energy for the surface explosion is equivalent to E_0. Since quantitative evaluation of the diffraction effect is difficult, E of the subsurface explosion is a parameter (range: $0.1E_0 \le E \le 0.5E_0$) in Figure 7. Our study shows that 30% of the high explosive ($E = 0.3E_0$) contributes to the generation and propagation of blast wave in the case of the subsurface explosion. We confirmed that the structural advantage of the subsurface magazine brings a strong mitigation of blast wave.

4. Conclusion

We performed numerical calculations to investigate the blast wave around a small-scaled model of a subsurface magazine.

The peak overpressure in the case of subsurface explosion agreed with the results of the experiment and was notably mitigated. Shock waves generated by a high explosive propagated in the circular pipe and reflected at the wall numerous times, causing a complex shock pattern

with a triple point in the vertical circular pipe. After the shock wave propagates to the exit of the subsurface magazine, the hemispherical blast wave expands. The peak overpressure distributions were reevaluated using a corrected scaled distance $Z^* = Z/(E/E_0)^{1/3}$ taking into account the energy loss by the subsurface magazine. Our study showed that 30% of the high explosive ($E = 0.3E_0$) contributes to the generation and propagation of blast wave in the case of the explosion inside the small-scaled model of a subsurface magazine.

References

1) T. Saburi, S. Kubota, K. Katoh, and Y. Ogata, Sci. Tech. Energetic Materials, 74, 53−60, (2013).
2) T. Saburi, S. Kubota, K. Katoh, and Y. Ogata, Sci. Tech. Energetic Materials, 74, 85−92, (2013).
3) T. Homae, K. Wakabayashi, T. Matsumura, and Y. Nakayama, Proceedings of Symposium on Shock Waves in Japan, 112−118, (2011) (in Japanese).
4) Y. Nakayama, K. Wakabayashi, T. Matsumura, and M. Iida, Applied Mechanics and Materials 82, 663−668, (2011).
5) Y. Sugiyama, K. Wakabayashi, T. Matsumura, and Y. Nakayama, Sci. Tech. Energetic Materials, 76, 14−19, (2015).
6) A. Harten, P.D. Lax and B. van Leer, SIAM Rev. 25, 35−61 (1983).
7) E.F. Toro, M. Spruce and W. Speares, Shock Waves 4, 25−34 (1994).
8) S.D. Kim, B.J. Lee, H.J. Lee, I.−S. Jeung, and J.−Y. Choi, Int. J. Numer. Meth. Fluids 62, 1107−1133 (2010).
9) C.N. Kingery and G. Bulmash, ARBRL−TR−02555, Ballistics Research Laboratory (1984).